Proceedings of ASME Turbo Expo 2011
GT2011
June 6-10, 2011, Vancouver, British Columbia, Canada

GT2011-46649

DISTRIBUTED PARAMETER ACOUSTIC MODELING OF A PERFORATION WITH BIAS FLOW

Alireza Mazdeh
University of Dayton
Dayton, Ohio, USA

Reza Kashani
University of Dayton
Dayton, Ohio, USA

ABSTRACT

Perforated acoustic liners (screech liners) with bias flow are commonly used for mitigation of thermoacoustic instabilities in augmentors. In addition to cooling the liner, the flow of air thru the liner perforation (dubbed 'bias flow') improves the damping effectiveness of the liner thru enhancing its energy dissipation. These liners are currently being designed using empirical design rules followed by build-test-improve steps, basically trial and error. The development of physics-based tools to assist in the design of such liners is of great interest to practitioners.

In this paper, the existing work in developing analytical, semi-empirical, and numerical techniques such as Large-Eddy Simulations (LES) in exploring the damping effectiveness of an acoustic liner with bias flow are reviewed. The paper continues with presenting the research in progress that has been conducted by the authors in this area with the goal of expanding the numerical modeling work beyond the current state of the art by including the variables that were not incorporated in previous studies including, but not limited to, hole orientation, combined effect of tangential grazing flow and bias flow interaction with acoustics, and different flow characteristics (Mach and Reynolds number). In addition, the spatial distribution of pressure and velocity over the aperture area (instead of the current practice of averaging these variables) are being looked at.

INTRODUCTION

Perforated acoustic liners (screech liners) are commonly used as the damping mechanism for mitigation of thermoacoustic instabilities in gas turbine engine applications. Such liners are typically arranged in such a way that the perforated skin of the liner in conjunction with the volume of the 'backing' form a reactive acoustic absorber. In addition to cooling the liner, the flow of air thru the liner perforation (dubbed 'bias flow') improves the effectiveness of the liner thru enhancing its energy dissipation; note that harmonic pressure differences across the perforations excite periodic vortex shedding, and shed vortices are convected away by the bias flow [1, 2]. This process converts the acoustic energy into mechanical energy, which eventually is dissipated into heat [3]. Considering the complexity of the associated turbulent aero-acoustic problem, research in this area has focused mainly on the study of a perforated plate (with bias flow) in the absence of interaction effects between neighboring perforations, leading to the study of a single perforation/aperture with periodic boundary conditions.

Theoretical and empirical approaches have provided the foundation for understanding the damping properties of liners but they are based on certain simplifying assumptions making them inadequate in addressing the more realistic conditions encountered in industrial applications. For instance, the sensitivity of acoustic properties of multi–perforated liners to the changes in the geometry and flow conditions cannot be studied easily using the above mentioned approaches. These limitations have shifted the direction of research toward numerical, more specifically numerical simulations using computational fluid dynamics (CFD) including, but not limited to, Large-Eddy Simulations (LES) and Scaled Adaptive Simulation (SAS) methods for studying damping behavior of liners. The first part of this paper summarizes the findings of the research conducted in the past 10-30 for comprehension of the acoustic-vortex interaction mechanism in the liners resulting in acoustic absorption. This includes some of the theoretical models quantifying acoustic Raleigh conductivity. In the second part of this paper, the acoustics of an orifice a single hole having a finite thickness, with bias flow is numerically simulated by solving the incompressible Navier-Stokes equations. The Raleigh conductivity across the aperture is evaluated using the average pressure and velocity over the aperture area and compared with the same data existing in the literature to examine some of the assumptions used in the previous works.

Summary of previous work

K_R defined as the ratio of mass flow rate to pressure drop across a single aperture [4]; see Equation (1). This quantity directly relates to the acoustic impedance Z, as shown in Equation (2).

$$K_R = \frac{\rho Q^{\bullet}}{\Delta \hat{P}} = \frac{j\rho\omega \hat{Q}}{\Delta \hat{P}} \tag{1}$$

$$Z = \frac{\Delta \hat{P}}{\hat{Q}} = j\frac{\rho A\omega}{K_R} \tag{2}$$

Inviscid and incompressible flows are the two core assumptions for calculating K_R analytically; the flow thru the aperture is presumed to be high Reynolds, low Mach number. The review of literature continues highlighting the limited available work on the use of computational fluid dynamic (mainly LES) methods in understanding the vortex creation/shedding mechanism in the context of acoustic absorption. Navier-Stoke equation for inviscid, incompressible flow, known as Euler equation, is written as:

$$\frac{\partial u}{\partial t} + (u.\nabla)u + \frac{\nabla p}{\rho} = 0 \tag{3}$$

In the absence of bias flow, contribution from the nonlinear term is negligible thus Equation (3) simply becomes:

$$\frac{\partial u}{\partial t} + \frac{\nabla p}{\rho} = 0 \tag{4}$$

By some manipulation, the relationship between pressure and mass flow rate, i.e., Raleigh conductivity K_R is found to be the ratio of area to length of the perforation; see Equation (5). For a circular hole with zero thickness, K_R equals to the aperture diameter:

$$K_R = \frac{A}{l_e} \tag{5}$$

Howe model [5]: Thru the use of vector properties Howe converted Euler equation into a form that contains vorticity term[1]; see Equation (6):

$$\frac{\partial u}{\partial t} + \nabla(\frac{1}{2}u^2 + \frac{p}{\rho}) = u \times \varpi \tag{6}$$

Defining Bernoulli enthalpy an important variable in acoustic as

$$h = \frac{1}{2}v^2 + \frac{p}{\rho} \tag{7}$$

By applying the divergence on Equation (7) while taking advantage of the interchangeability between partial and divergence results in:

$$\frac{\partial}{\partial t}(\nabla.u) + \nabla^2 h = \nabla.(u \times \varpi) \tag{8}$$

[1] In the presence of bias flow, it is no longer easy to derive a relationship between mass flow rate and pressure, directly.

By taking into account the incompressibility of the fluid, one more time:

$$\nabla^2 h = \nabla.(u \times \varpi) \tag{9}$$

Howe linearized Equation (9) using the perturbation theory (by viewing the variables as the sum of their fluctuating and mean values, i.e. $\omega = \overline{\omega} + \varpi$; $u = \overline{U} + u'$) and arrived at:

$$\nabla^2 h = \nabla.(\overline{U} \times \varpi') \tag{10}$$

Approximating shed vorticity by $\varpi' = \sigma k\delta(r-R)\exp(-jw(t-x/U_0)$ and placing it into Equation (10) Howe came up with an equation for Bernoulli enthalpy h in cylindrical coordinate system which is mathematically classified as inhomogeneous, axi-symmetric Laplace equation. Solving that equation enabled Howe to find a relationship between mass flow rate and pressure which in turn resulted in an expression for Raleigh conductivity of a single hole with bias flow for a very thin plate:

$$K_R = \gamma - i\delta = 1 + \frac{\frac{\pi}{2}I_1(Sr)e^{-St} - jK_1(Sr)\sinh(St)}{St[\frac{\pi}{2}I_1(Sr)e^{-St} + jK_1(Sr)\cosh(St)]} \tag{11}$$

$$Sr = \frac{2\pi fa}{U} \tag{12}$$

Howe's model was developed based on linear sound absorption theory. He also assumed large aperture spacing/radius so that no interaction between apertures occurs. Howe's model has been extensively studied by many researchers working in the field of acoustic damping and verified by a series of experiments.

Modified Howe model [6]: Realizing the impact of the thickness of the perforation on its acoustic properties, Jing and Sun modified Howe's model by adding impedance due to the thickness (Z_{th}) to the impedance due to the bias flow (Z_{bf}) and defined the total impedance Z_t in their model as:

$$Z_t = Z_{th} + Z_{bf} \tag{13}$$

Consequently mathematical expression for modified Howe conductivity (K_{RM}) is found by:

$$\frac{1}{K_{RM}} = \frac{1}{K_{Rth}} + \frac{1}{K_{Rbf}} \tag{14}$$

K_{Rbf} and K_{Rth} are the corresponding acoustic conductivity due to the thickness and bias flow accordingly. Substituting for K_{Rbf} and K_{Rth} from Equations (11) and (5) in Equation (13) results in Raleigh conductivity known as modified Howe model in the literature:

$$K_{RM} = 2a\left(\frac{1}{\gamma - j\delta} + \frac{2}{\pi}\frac{l_e}{a}\right)^{-1} \quad (15)$$

Although there is no theoretical basis for modified Howe model, this model is widely used when the thickness of the perforation cannot be ignored. The real and imaginary parts of the Raleigh conductivity predicted by the Howe model of Equation (11) and modified Howe model of Equation (15), for a perforation with $\overline{T}$ =0.5, are presented graphically in Figure 1. Clear from Figure 1, modified Howe model predicts reduction in acoustic conductivity of the perforated plate at Strouhal numbers slightly greater than unity. The two models basically have the same form only the peak in imaginary part of K_R shows a slight shift to the right, due to the thickness effect, in the modified model.

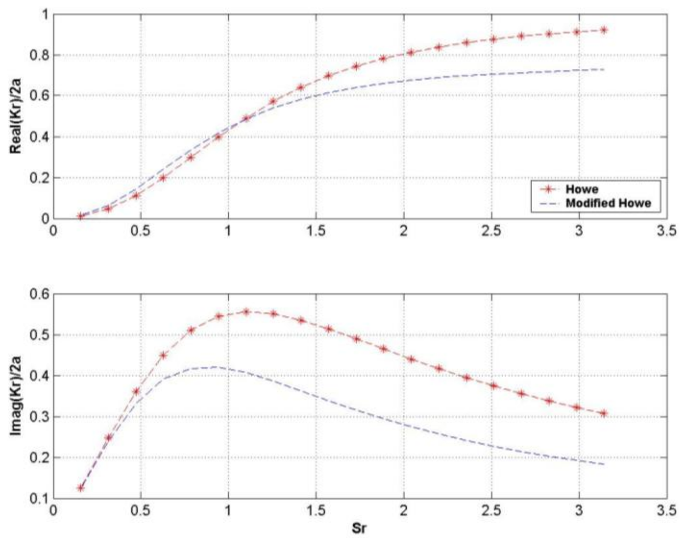

FIGURE 1 REAL AND IMAGINARY PARTS OF K_R OF A SINGLE APERTURE WITH $\overline{T}$ =0.5, REPRESENTED BY HOWE AND MODIFIED HOWE MODELS

Jing Sun numerical model [7]: Subsequent to modifying Howe's model to account for the thickness, Jing and Sun took a more accurate approach to account for the perforation thickness. They started from the governing equation derived by Howe and applied it to a model with finite thickness. This more elaborate model has a fundamental difference with the original work of Howe as it assumes a more complex form for the jet profile by using the geometry of the free streamline obtained from experimental data [8]. This is in contrast to Howe's model which assumes a simple cylindrical vortex sheet; see Figure 2. All the other assumptions are similar to those of Howe's. Due to the complex jet profile assumption, Jing and Sun were not able to solve the governing equation analytically and had to use the boundary value method to numerically solve the equation. They solved their numerical models for several cases of thickness/radius ratios of $\overline{T}$ = 0, .5, 1.0, 1.5 and 2. Figure 3 depicts the graphical representation of these solutions. The fact that their results reduce to those of Howe's in the limit of zero thickness gives more credibility to their data.

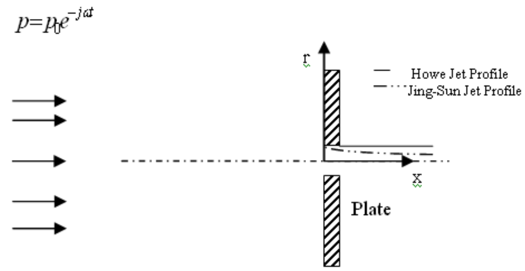

FIGURE 2 BIAS FLOW CONFIGURATION AND THE JET PROFILE USED IN [7]

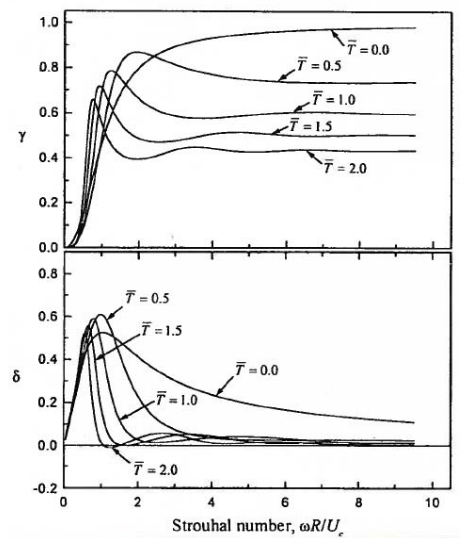

FIGURE 3 REAL AND IMAGINARY PARTS OF K_R FOR DIFFERENT THICKNESS/RADIUS RATIOS [7]

Jing and Sun compared their results with modified Howe as well as experimental data. They observed better agreement between experimental data and the prediction of their numerical model than with the prediction of modified Howe model. Noticeable, sharp peaks in K_R predicted by Jing and Sun, that is absent in the result of Howe and modified Howe, distinguishes Jing-Sun's model from Howe models. The occurrence of this sharp peak seems to be geometry dependent as it is a function of thickness/radius ratio. Jing and Sun provided no explanation for this drastic behavioral change.

Overview of previous LES works

By recent advancements in the computer hardware and software technologies the use of fine grid size and time step, as well as the large number of time steps[2] in solving unsteady Navier Stokes equations are becoming a possibility. Having said this, capturing all scales of the turbulent fluctuation,

[2] Fine grid and small time stepping are required to generate statistically meaningful correlations for the fluctuating components.

including small and large, known as Direct Numerical Simulation (DNS), is still out of reach for the near future [9]. The next approximation level which is more promising for industrial applications is LES, where only the turbulent scales larger than the grid size are calculated. This approach is similar to DNS, except that the smaller scales are filtered and are not calculated by direct discretization and instead are accounted for by mathematical models.

LES has been used for modeling complex flows such as the ones associated with combustion instabilities. Despite this, LES is still a new avenue for studying damping properties of multi-perforated liners. Besides, the excessive need for CPU time and memory requirement by LES make this technique too demanding for building complicated models that include all the complexities associated with the geometry and flow of industrial sized liners with multiple interacting holes with jet flow. As such, in all the LES work associated with studying the acoustic damping of liners, it has been assumed that the perforations are spaced out far enough from each other that their interactions can be ignored. With this assumption, only one perforation is normally modeled and via the use of periodic boundary condition, the outcome of study is extended to a liner with multiple holes.

A very recent work by Mendez et. al. [10] used LES to confirm damping properties of liners with bias flow; the configuration used in this work is shown in Figure 4. Among Howe, modified Howe, Jing-Sun and also Bellucci [11] experimental data, Mendez et. al. [10] LES data has the most agreement with numerical model developed by Jing-Sun [7].

The very good agreement between the jet profile obtained by LES and the jet profile found experimentally by Rouse and Abul-Fetouh [8], which was used in Jing-Sun model, especially at the beginning of the separation allowed Mendez et. al. [10] to explain the good correlation they observed between their LES results and the predictions by the Jing-Sun model. While their work clearly showed how numerical simulation can effectively be used to evaluate assumptions it also underlines the importance of the accurate jet profile ignored in Howe model and signify the lack of reliability associated with the experimental evaluation of the acoustic properties of liners with small size apertures.

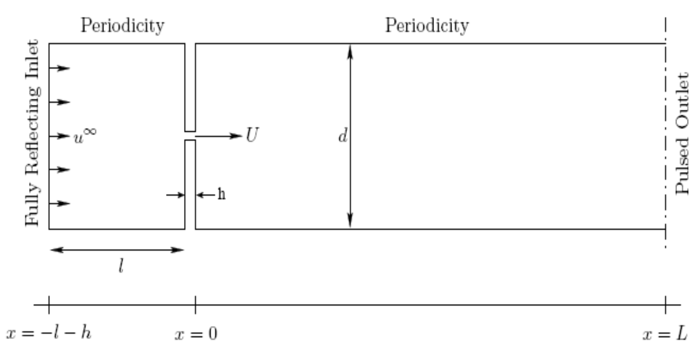

FIGURE 4 CONFIGURATION USED BY [10]

The primary focus of Mendez et. al. [1] work was to observe acoustic attenuation properties of perforated plate thru the use of LES as an alternative way to empirical and analytical models. They accomplished this by evaluating acoustic quantities such as reflection coefficient and absorption coefficient from their LES model. Although these acoustic properties are easily related to Rayleigh conductivity but Mendez et. al. [10] approach to study damping properties of the perforated plates does not extract Rayleigh conductivity directly from the LES model.

Another work in this area which also uses LES is done by Eldrige et. al.[12]. Contrary to Mendez et. al. [10] approach Eldrige et. al. [12] calculates Rayleigh conductivity directly from the LES model. Their geometry, shown in Figure 5, is substantially different from those used in previous analytical and experimental studies as they used a configuration more in line with practical film cooling liners. Their model includes grazing turbulent flows in the regions above and below the aperture. They used a tilted aperture (shown in Figure 5) that also has relatively large thickness/radius ratio ($\overline{T}$ =8). Eldrige et. al. [12] only compared their data with modified Howe model as no Jing-Sun data is available for ($\overline{T}$ >2) in the literature.

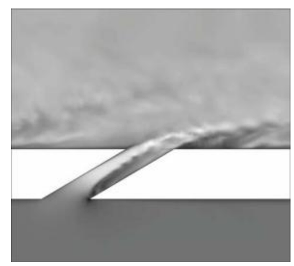

FIGURE 5 TILTED CYLINDRICAL APERTURE USED BY [12]

Although Eldrige et. al. [12] showed good agreement at lower frequencies with modified Howe model, but their work cannot provide a solid conclusion due to the drastic differences between their geometry and flow with those in the modified Howe model. The good agreement could be the result of large thickness/radius ratio used in his model. In fact the notion of adding impedance by the thickness and bias flow used in modified Howe model might be justified for very large values of thickness/radius ratio. If this is true it will indicate that thickness plays a more dominant role for perforations with larger thickness/radius ratio.

The two works discussed above and others that might be available in the literature use mostly non-commercial CFD codes developed in-house that use higher order differencing schemes, than the ones available in commercial packages which mostly offer second order differencing schemes [13]. Despite the limitations on the differencing capabilities of commercial CFD tools, their adaptation in exploring the impact of bias flow in the acoustic damping effectiveness of liners would encourage the use of LES or similar tools by the practitioners who prefer the numerical robustness offered by the commercial CFD codes than the high order differencing capabilities offered by the in-house codes. In the study reported below, ANSYS CFX is used to do just that.

NUMERICAL SIMULATION STUDY

With the goal of expanding the numerical modeling work beyond the current state of the art, the authors are planning to include the variables that were not incorporated in the above-mentioned studies. Such variables include, but are not limited to, hole orientation, combined effect of tangential grazing flow and bias flow interaction with acoustics, and different flow characteristics (Mach and Reynolds number). As the first step toward achieving this goal, a configuration similar to the one used by Mendez et.al. [10] (shown in Figure 6) is modeled. Moreover, only bias flow is considered in this study; grazing flow is not included in the analysis.

LES approach is still impractical for many engineering calculations because of the fine grid size and time step requirements, as well as the large number of time steps required to generate statistically meaningful correlations for the fluctuating components. The method with highest level of approximation for time dependent flows is the Unsteady Reynolds-averaged Navier-Stokes (URANS). These methods are applied for unsteady flows when the turbulent level is not very large. Even for small turbulent level, LES clearly can show more small-scale unsteady vortical structures than the URANS model. This is because the URANS only represent the ensemble averaged flow field and hence can only exhibit periodic large-scale unsteadiness while the LES represents an instantaneous snapshot of the flow field. New unsteady approaches for performing accurate CFD have been developed by researchers with the intension to preserve the accuracy while avoiding putting extreme demands on computer resources. These intermediate models are called Hybrid and their approximation ranks between LES and RANS. Scaled Adaptive Simulation (SAS) and Detached Eddy Simulation (DES) are two of such methods. Hybrid model solves the RANS equations in the attached boundary region and switches to a LES model for detached flow regions [14]. DES is the 1st industrial model of high Re flows with LES content, it is an explicit mix of RANS and LES, it performs the switch from the RANS to LES by a comparison of the turbulent length-scale calculated by RANS; this produces grid dependency in the model. Then SAS was developed to overcome this concern by allowing the model to automatically adapt to the length scale present in the flow [15]. This is substantially different from a DES simulation as it does not explicitly split up the flow in RANS and LES region.

The excessively large number of grid points[3] required for accurate LES, using low-order differencing available in CFX, proved too demanding for the 8 node processor available to us. As such, we have pursued the use of SAS, in place of LES. To stay consistent with the assumptions used in theoretical models incompressible flow which is less involved computationally is used. Similar to Howe's theoretical model, the infinite configuration is applied by the use of the periodicity boundary conditions. By applying periodicity, a single jet is modeled isolated from other jets and without any impact from the surrounding walls. Periodic conditions are applied in both directions tangential to the plate so that only one micro-jet is computed; this allows reducing the computational domain to only one perforation. Flow conditions, boundary conditions, and model geometry are shown in Figure 6.

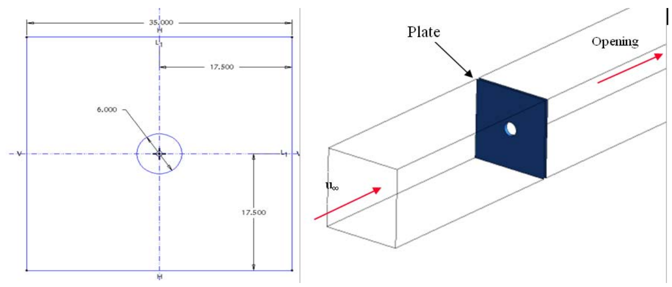

FIGURE 6 MODEL CONFIGURATION, PLATE DIMENSION AND FLOW CONDITIONS: H= 1.5 mm; a=3 mm; d = 35 mm; $\sigma = \pi a^2/d^2 = 0.0231$; $U_\infty = 0.115$ m /S; $U_O = U_\infty/\sigma = 5$ m/S; FLOW CONDITIONS: M =0.015 AND Re=2055

Excitation is done either by modulating the pressure difference across the plate and computing the resulting oscillations in volume flow rate, or by modulating the imposed bias flow and computing the resulting pressure oscillations. It is preferred to apply the excitation by mass flow and measure the pressure difference across the hole; as it is easier to assess model quality. Mass flow fluctuation of 2% is added to the mean flow at the inlet in from of:

$$Q = \overline{Q} + \hat{Q}\cos(\omega t) \tag{16}$$

Pressure differential across the plate follow the same harmonic variation, i.e.,

$$P^+ - P^- = \Delta\overline{P} + \Delta\hat{P}\cos(wt + \theta) \tag{17}$$

The average value is removed when calculating the Rayleigh conductivity thus the dynamic pressure drop across the hole is simply defined as:

$$P^+ - P^- = \Delta P\,\mathrm{Re}\{e^{j\theta + wt}\} < 0 \tag{18}$$

P^- is the spatial average of pressure at entrance of the hole, P^+ is the spatial average of pressure at exit of the hole and θ is the phase difference of pressure drop signal with respect to the input signal (mass flow).

[3] Second order central differencing in space and 2nd order backward differencing in time [13]

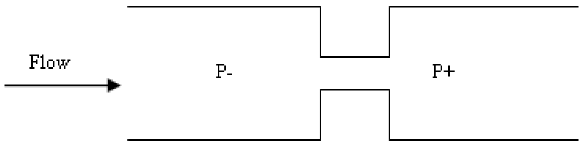

FIGURE 7 PRESSURE DROP DEFINITION

After substitution for mass flow and pressure drop in Equation (1) and cancelling e^{jw}; K_R is calculated directly in terms of fluid quantities.

$$K_R = \frac{j\omega\rho\hat{Q}}{P^+ - P^-} = j\frac{\omega\rho\hat{Q}}{\Delta P e^{j\theta}} = \frac{\omega\rho\hat{Q}}{\Delta P}(j\cos\theta + \sin\theta) \tag{19}$$

Due to the frequency dependency of K_R, the frequency of harmonic perturbation added to the inlet needs to vary. Neither CFX nor any other CFD tools can provide the computation in the frequency domain, so for each frequency point a simulation in time domain is needed to collect $\hat{Q}$, ΔP and θ. In the range of 50-850 Hz, with the steps of 100Hz, nine frequency points are selected for transient runs. The simulation time is chosen based on achieving statistical convergence in the data. A physical time of 15 periods is chosen for simulation time of each run. Converged statistics is achieved after 10 periods. During data extraction the transitory part is ignored and the data from the last 5 cycles is used. Another important parameter in the simulation is Δt which needs to be specified very cautiously. CFX is an implicit code [13] and can therefore converge on CFL $= C\Delta t/\Delta y$ greater than one or larger time step sizes. However, for accurate transient calculations and not to overly damp the turbulence a small CFL is advised but it should not be unnecessarily too small to add more CPU time. Time stepping is modified to adapt time-step size dynamically to keep the CFL constant. This will resolve some of the practical issues regarding disc space and CPU time. After intensive computational settings re-evaluations a CFL of 0.2-0.25 seems to accomplish acceptable accuracy in an affordable CPU time. These steps are all required in advance to administrate a very efficient and economical time marching in pursuing an accurate solution. As to the element type, full hex and full tetrahedral and tetrahedral with prism for the boundaries have been tried but only full hex mesh seems to work the best for our calculations. Typical mesh plots are presented in Figure 8.

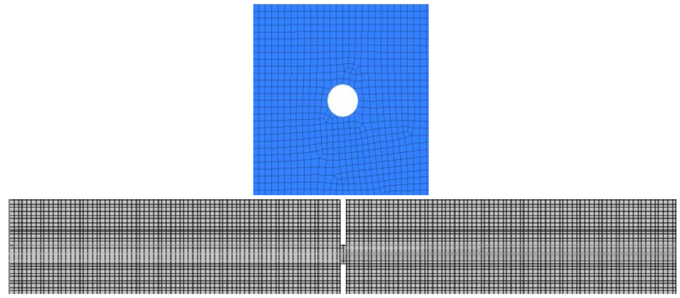

FIGURE 8 MESH PLOTS OF THE COMPUTATIONAL FLUID DOMAIN, DIFFERENT CROSS SECTION VIEWS

RESULTS AND DISCUSSION

Before discussing the results it is important to draw up a strategy for evaluating the results. First, to ensure the equality of the mean volume flow, we need to check for having the continuity condition at the inlet to the computational domain and at the hole is met. In the case of incompressible flow, fluctuation level at these points should be equal. Moreover, there should be no phase difference for volume flow between these locations [16]. Data shown in Table 1 are the raw data directly from CFD model, summarizing the fluid quantities measured from the model. Err1 is defined as the difference between the 'volume flow' at the inlet and at the aperture, i.e., the measure of how well the continuity condition is met. The nonzero values of Err1 may be due to the discretization error or introduction of flow at the side wall boundaries, unintendedly. Note that for very weak forcing, the error in global conservation of mass may become comparable to the forcing amplitude, but if physics is correctly implemented, this error should be reduced by using a finer grid. The 5-6% offset seems to be consistent for different pulsation frequencies leading us to believe that it is because of discretization error. The incompressibility assumption is measured by Err2 defined as phase deviation of volume flow at the aperture from that at the inlet; it is worth noting that although for all frequencies it is less than 1 degree but as the frequency increases this deviation increases.

The two traces in Figure 9 depict the typical CFD outputs and its curve fits for a sample excitation frequency. Figure 10 presents the real and imaginary components of Rayleigh conductivity; these data are normalized to the Rayleigh conductivity of no bias flow. Finally Figure 11 presents normalized specific impedance of a single aperture for different Strouhal numbers.

Table 1: CFD RESULTS

f (Hz)	$\Delta\hat{P}$ (Pa)	$\theta_{\Delta\hat{P}}$ (°)	Err1= $1-(\hat{Q}_{hole}/\hat{Q}_{inlet})$ ** %	Err2= $\theta_{\Delta\hat{Q}}$ * (°)
50	1.18	-180.3	6	-0.2
150	1.13	-172.1	6	-0.1
250	1.02	-158.1	6	-0.2
350	1.03	-137.2	6	-0.4
450	1.27	-118	5	-0.4
550	1.69	-108.5	5	-0.5
650	2.12	-104.3	5	-0.5
750	2.58	-104.1	5	-0.4
850	2.98	-103.5	5	-0.6

* This is the phase of the volume flow at the hole with respect to inlet flow; theoretically it has to be zero

**Data in this column theoretically represents error as it should equal to zero

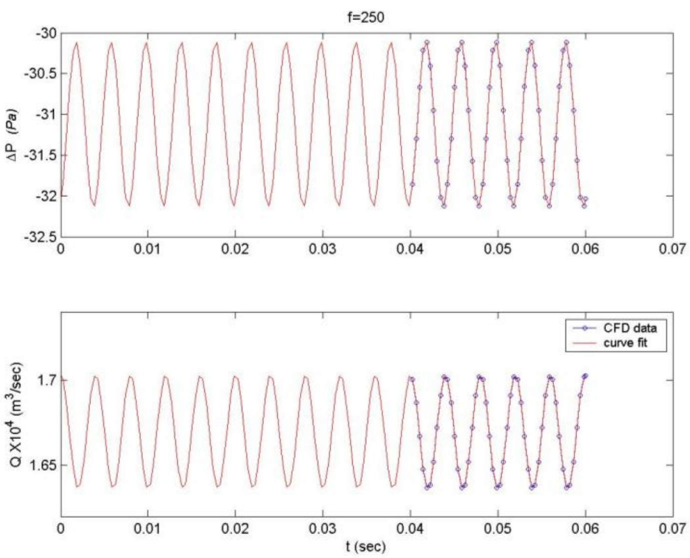

FIGURE 9 TYPICAL FLOW RATE AND PRESSURE DROP PLOTS FOR A SAMPLE FREQUENCY PULSATION OF 250 Hz

Our data show the best agreement with Jing-Sun numerical model as it takes into account the geometry of aperture and jet shape. It is important to note that modified Howe has the least agreement among all the models used in the comparison in this study (which was carried out for thickness to radius ratio of. $\overline{T} = 0.5$). It might be too early to draw a conclusion without conducting more studies, but it seems that at lower $\overline{T}$ s the behavior of the model can be described better by Howe and at higher values of $\overline{T}$ it is better described by modified Howe.

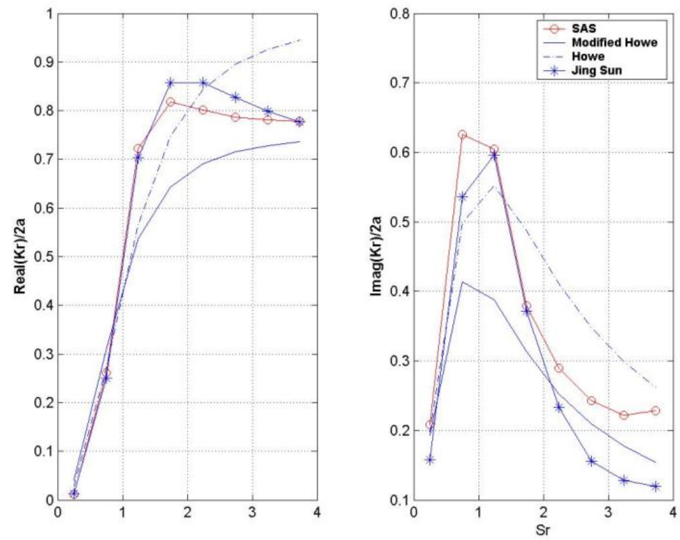

FIGURE 10 REAL AND IMAGINARY REPRESENTATION OF THE NORMALIZED ACOUSTIC CONDUCTIVITY VERSUS STROUHAL NUMBER

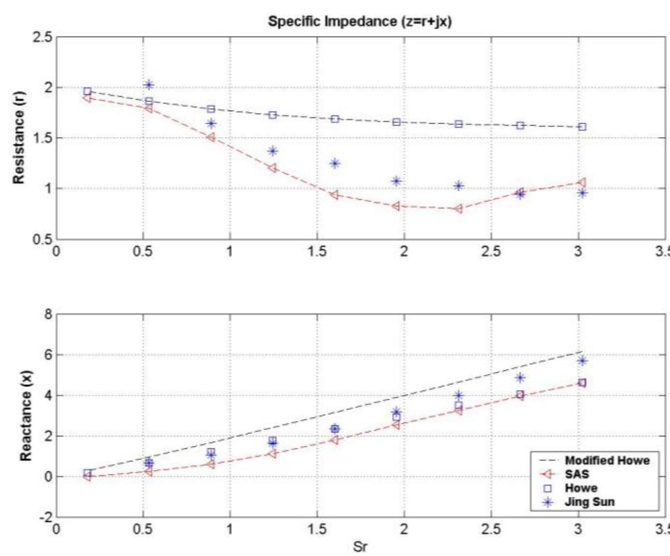

FIGURE 11 NORMALIZED SPECIFIC IMPEDANCE OF A SINGLE APERTURE VERSUS STROUHAL NUMBER

SUMMARY

The existing analytical, semi-empirical as well as Large-Eddy Simulations (LES) based numerical tools in exploring the damping effectiveness of an acoustic liner with bias flow are reviewed. In addition, the analytical and semi-empirical approaches are put to numerical simulation test, the results of which indicate their verification under the restricting assumptions they were developed for. We are currently expanding the numerical modeling work beyond the current state of the art by including the variables that were not incorporated in previous studies including, but not limited to, hole orientation, the combined effect of tangential grazing flow and bias flow on the acoustics, and different flow characteristics (Mach and Reynolds number). In addition, we are looking at the spatial distribution of pressure and velocity over the aperture area (instead of the current practice of averaging these variables). The results of these studies will be presented, as they become available, in future papers.

ACKNOWLEDGMENTS

The authors are very grateful for the guidance of Dr. Michael White and Dr. Barry Kiel of The Air Force Research Laboratories at Wright Patterson Air Force Base, in the conduct of this study. It would not have been possible without their help.

NOMENCLATURE

$\hat{Q}$ *:Flow fluctuations Amplitude*
ΔP: Pressure fluctuations Amplitudes
Sr: Strouhal number
U_0: Mean flow velocity
Re: Reynolds's Number
I_1,K_1: Modified Bessel functions
f : Excitation frequency
ρ: Density
a: Radius of aperture
K_R: Raleigh conductivity
ω': Shed vorticity
ω: Angular frequency
u: Velocity
A: Cross section area of aperture
$\bar{T}$ *:Thickness/radius ratio*
$\bar{Q}$ *:Mean volume flow*
D: Hole spacing
u_∞ : Inlet Velocity
M: Mach Number
C: Speed of sound
σ: Plate porosity
Z: Impedance
t: Time
h: Bernoulli enthalpy
Δt: time step size
Δy: grid size
CFL: Courant numbers
$Q^\bullet$ *: Volume flow rate*
Q: Volume flow
l_e : hole effective length

REFERENCES

[1] Howe, M.S., 1998 "Acoustics of Fluid-structure Interactions", Cambridge University Press,

[2] Bechert, D. W, 1980 "Sound absorption caused by vorticity shedding, demonstrated with a jet flow" J. Sound and Vibration, Volume (70), Issue 3, p. 389-405

[3] Eldredge, J. D & Dowling, A.P, 2003. "The absorption of axial acoustic waves by a perforated liner with bias flow" J. Fluid Mech. Vol. (485) pages 307-335

[4] Rayleigh, L., 1945. "The theory of sound", vol. 2 New York: Dover

[5] Howe, M.S. 1979. "On the Theory of Unsteady High Reynolds Number Flow Through a Circular Aperture" Proceedings of the Royal Society of London Vol. 366, No. 1725, pp. 205-223

[6] Jing, X.D. Sun, X.F. 1999. "Experimental investigations of perforated liners with bias flow," Journal of the Acoustical Society of America , Vol. 106, No. 5, pp. 2436–2441

[7] Jing, X.D. Sun, X.F. 2000 "Effect of plate thickness on impedance of perforated plates with bias flow," AIAA Journal 38 1573–1578

[8] Rouse, H. and Abul-Fetouh, A. "Characteristics of irrotational flow through axially symmetric orifices," Journal of Applied Mechanics 17 (1950) 421–426

[9] Hirsch, C., T. D., 2002 "Numerical Computation of Internal and External Flows, Computational Methods for Inviscid and Viscous Flows," 2nd ed., Wiley Series in Numerical Methods in Engineering

[10] Mendez, S. & Eldredge, J. D., 2009 "Acoustic modeling of perforated plates with bias flow for Large-Eddy Simulations," Journal of Computational Physics, Vol. 228(13), pages 4757-4772

[11] Bellucci, V., Paschereit, C.O., and Flohr, P., 2002 "Impedance of perforated screen with bias flow," AIAA Paper 2002-2437,

[12] J. Eldredge, M. Shoeybi and D. Bodony., 2006 "Numerical investigation of the acoustic behavior of a multi-perforated liner" Proceedings of the 2006 Summer Program, Center for Turbulence Research, Stanford University

[13] CFX manual, the Theory and the solver, Software Package, Version 04, 275 Technology Drive Canonsburg, PA 15317

[14] A Scale-Adaptive Simulation Model using Two-Equation Models F.R. Menter1 and Y. Egorov2 ANSYS CFX Germany, 83624 Otterfing, Germany

[15] AIAA 2003-0767 A Scale-Adaptive Simulation Model for. Turbulent Flow Predictions F.R. Menter, Kuntz and R. Bender CFX Germany Otterfing Germany

[16] Panton, R. L. "2005 'Incompressible flow", Wiley, John & Sons, Incorporated,

